2019-06-20

Mechanical properties and microstructure analysis of FA-GGBS-HMNS based geopolymer concrete

Li, Long-yuan

10.1016/j.conbuildmat.2019.03.202
Construction and Building Materials
Elsevier

Received 20 November 2018, Accepted 15 March 2019.
Construction and Building Materials 210: 198-209.
https://doi.org/10.1016/j.conbuildmat.2019.03.202

Mechanical properties and microstructure analysis of FA-GGBS-HMNS based geopolymer concrete

Aissa Bouaissi[1], Long-yuan Li[1], Mohd Mustafa Al Bakri Abdullah[2,3], Quoc-Bao Bui[4]

(1) School of Engineering, University of Plymouth, Plymouth PL4 8AA, UK
(2) Center of Excellence Geopolymer and Green Technology, Universiti Malaysia Perlis, Perlis 01000, Malaysia.
(3) School of Materials Engineering, Universiti Malaysia Perlis, Perlis 01000, Malaysia.
(4) Faculty of Civil Engineering, Ton Duc Thang University, Ho Chi Minh City, Vietnam.

Corresponding author's contacts
Email: aissa.bouaissi@plymouth.ac.uk , Phone: +447498479367
Address: School of Marine Science and Engineering, University of Plymouth, PL4 8AA, UK

Abstract - This paper presents an experimental investigation on the mechanical properties and microstructure of geopolymer concrete mixed using class F fly ash (FA), ground granulated blast-furnace slag (GGBS) and high-magnesium nickel slag (HMNS). An optimal combination of FA, GGBS and HMNS was determined using the compressive strength tests of geopolymer (GP) pastes mixed with various different replacements of FA with GGBS and/or HMNS. It was found that the replacement of FA with 20% of GGBS and 10% of HMNS in GP concrete increases the 28-day compressive strength by 100% and the 28-day splitting tensile strength by 58%. The microstructure analysis of the GP concrete using SEM, XRD, and FTIR showed the formation of aluminosilicate amorphous phase in a three-dimensional network. The SEM images revealed a fully compact and cohesive geopolymer matrix, which explains the reason why the mechanical properties of the FA based GP concrete with both GGBS and HMNS are improved.

Keywords: Fly ash; ground granulated blast-furnace slag; nickel slag; geopolymer; mechanical property; microstructure.

List of notations

ECO_2	embodied carbon dioxide
EE	embodied energy
FA	fly ash
FTIR	Fourier transform infrared spectroscopy
GGBS	ground granulated blast furnace slag
GP	geopolymer
HMNS	high-magnesium nickel slag
PC	Portland cement
SCM	supplementary cementitious material
SEM	scanning electron microscope
XRD	x-ray diffraction

1. Introduction

Concrete, owing to its availability, easy preparation and fabrication, is the most popular construction material. Today, concrete is the second most used material after water, with nearly three tonnes used annually for each person on earth. In terms of its effectiveness, price and performance when considered for most purposes, none of the other materials could compete or replace concrete. However, the production of ordinary Portland cement (PC) concrete requires a large embodied energy (EE) and produces a large amount of embodied carbon dioxide (ECO_2). It was reported that depending upon the type and method of mix design, to produce one tonne of PC concrete requires roughly 150-250 kWh EE and produces approximately 75–175 kg ECO_2 [1,2]. In addition, PC concrete is a composite material, composed of aggregates embedded in a hard matrix of cement paste that fills the space among the aggregate particles and glues them together. PC production is highly energy intensive next only to steel and aluminium and its EE is very high at about 1300 kWh/tonne; further, a tonne of PC production causes the emission of around 0.8 tonnes of the green gas CO_2 [3,4]. Therefore, an urgent task of research is to find alternatives to reduce or even replace the PC in concrete to make the concrete industry more eco-friendly.

Numerous studies have been carried out in the last two decades to pursue and support the concept of environmentally friendly blending materials. The work involves the use of supplementary cementitious materials (SCMs) such as fly ash, slag and other pozzolanic materials to partially replace PC [5,6] when manufacturing PC concrete products, and the development of low carbon concretes such as the geopolymer (GP) concrete [7,8] that does not use PC. Similar to the PC concrete, GP concrete also consists of a binder made from fine powdery materials, called as geopolymers, the bulk volume filling granular particles made of aggregates, and a liquid component of the mix made of alkaline chemicals. At present, fly ash (FA) appears to be the most promising source material for the large-scale industrial production of GP concrete due to its favourable rheological properties and lower water demand when mixed with aggregates and alkaline solutions [9,10], although the other by-product materials such as silica fume, slag, rice-husk ash, and red mud and other natural minerals such as kaolinite, clays, micas, andalousite, spinel could also be used as the source materials.

FA is a by-product of coal-fired thermal power plants. It primarily contains silica, alumina, iron oxide, and lime [11]. ASTM C618 [12] classifies FA into two categories, class F and class C. The former is produced from anthracite and bituminous coal and contains less than 5-10% lime, which is essentially a pozzolanic material, meaning that it does not react with water on its own, but reacts with calcium hydroxide in the presence of moisture to give calcium silicate hydrates. The latter is normally derived from lignite and sub-bituminous coal and contains a high amount of lime (15-30%). Apart from its pozzolanic property, class C FA also has a cementitious property. It can react with water on its own to form calcium silicate hydrates. Class F and class C FAs have both been used as SCMs in PC concrete with up 40% replacement of PC by mass [12]. However, when used as the precursor in GP concrete it is more effective to use class F FA than class C FA.

The use of FA to produce GP concrete has been investigated extensively in recent years. The work involves the mechanism of geopolymerization, the mechanical properties and durability of the resulting concrete, and the effect of using different binder materials on the mechanical properties of GP concrete. For example, Palomo et al. [13] conducted an experimental study on blended cement containing 30% PC clinker and 70% FA. The powdery material was mixed with deionised water for “normal” hydration, and with two different alkaline solutions for “normal” alkaline activation. It was found that the mechanical strength developed by this highly blended cement differed considerably depending on the hydrating solution used. Bouzoubaa et al. [14] presented a study on the mechanical properties and durability of concrete made with a high-volume FA blended cement using a coarse FA that does not meet the fineness requirement of ASTM C 618. The results were compared with those of the high-volume FA concrete in which unground FA had been added in the concrete mixer. In their study, the properties of the fresh and hardened concrete including durability were investigated. The obtained results showed that the fabricated concrete which had blended with cement had better mechanical properties and durability than the concrete made with the addition of the unground FA. Olivia and Nikraz [15] provided a study on the mechanical properties and durability of concrete produced from the optimal mixes of FA-based GP mixtures. The results showed that the geopolymer concrete could achieve a 55 MPa compressive strength within 28 days and could have higher mechanical properties including tensile and flexural strengths. The FA-based GP concrete also showed a significant improvement in other mechanical properties by producing less expansion and drying shrinkage compared to those of OPC control mix. However, it was reported that there is a significant change in the compressive strength of all geopolymer mixes at each wetting-drying cycle with higher weight losses compared

to that of OPC concrete. Chi and Huang [16] investigated the mechanical properties and binding mechanism of FA-slag based GP mortars. The work involves the compressive strength test, flexural strength test, water absorption test, drying shrinkage test, scanning electron microscopy (SEM) and x-ray diffraction (XRD) analysis of GP mortars. The test results showed that the binding mechanism and properties of FA-slag based GP mortars were significantly influenced by both of fly ash to slag ratio and the dosage of sodium oxide (Na_2O). In addition, the SEM and XRD analysis revealed that the hydration products of FA-slag based GP mortars mainly consist of amorphous alkaline aluminosilicate and low-crystalline calcium silicate hydrate gel. Except for drying shrinkage, better mechanical properties including the compressive strength, flexural strength and water absorption, were obtained in FA-slag based GP mortars in comparison with those of OPC mortars. Albitar et al. [17] reported an experimental study on the behaviour of GP concrete in both its wet and hardened states using Class F FA. The experimental programme included 15 mixing designs to examine the influence of water-to-binder and superplasticiser-to-binder ratios on the workability and strength of FA-based GP concrete. Velandia et al. [25] investigated the effect of mix design, curing conditions and engineering properties on the long-term properties of Na_2SO_4-activated high volume fly ash concrete. The results showed that using Na_2SO_4 as a chemical activator initiates chemical reactions in the mixture, which leads to an increase in its alkalinity and the acceleration of FA dissolution, which in turn increases the matrix density due to the formation of more ettringite.

Note that, apart from FA, there are many other industrial wastes that need to be recycled [18]. Therefore, there is a need to develop suitable alternatives to FA to promote commercialisation of GP concrete technology. Among many industrial by-products, ground granulated blast-furnace slag (GGBS) and high-magnesium nickel slag (HMNS) are the two materials which have been found to be able to improve the performance of resultant GP concrete when they are used to partially replace FA [19,20]. GGBS is a by-product obtained from iron industries when cooled and ground to the fineness of cement. GGBS has hydraulic properties. ASTM C 989 [21] grades blast furnace slag into grades 80, 100, and 120 according to its hydraulic activity, with the higher grade contributing more to strength potential. GGBS has been used as an SCM in PC concrete for many years, either as a mineral admixture or a component of blended cement [22,23]. The use of GGBS in PC concrete can decrease the long-term drying shrinkage of concrete and improve the workability of fresh concrete and the long-term strength and durability of the hardened concrete. It has been reported that the use of electric furnace ferronickel slag (FNS) as a filler aggregate in

the production of PC and GP concretes can improve their strength and durability. Some research showed that the use of 20% of FNS powder in geopolymer exhibited better strength and durability properties when compared to 100% FA based geopolymer [26]. Cao et al. [27] investigated the possibility of using FNS mixed with GGBS to manufacture alkali-activated cements. Their results showed that there was no influence on the setting times when the FNS used up to 40%; however, mixing 60% of FNS prolonged the setting times and significantly decreased the mechanical strengths. Another study was reported on the effect of using a mix of furnace nickel slag (FNS) and phosphorous slag (PS) on the hydration and hardening processes, mechanical and durability properties of the concrete [28]. The results showed the superior mechanical properties and permeability to chloride ions of the FNS and PS concrete mixture compared to that of high volume FA concrete [28].

HMNS is also an industrial by-product, produced from nickel production from high-magnesium nickel oxide ores. It contains considerable amounts of silica, alumina and magnesium. In most countries, HMNS is normally treated as an industrial waste material and is stored by landfill, which essentially has a hazardous effect on ground and ground water. Therefore, it is important to seek a way by which the HMNS can be recycled. Recently, Yang et al. [24] presented an experimental investigation on the use of HMNS and its effect on the reaction, mechanical properties and microstructure of FA-based geopolymers when HMNS was used as a partial replacement of FA. The results showed that the use of 20% HMNS substitution results in the highest compressive strength and the lowest linear drying shrinkage.

In this paper, an experimental investigation is reported on the mechanical properties and microstructure of GP concrete mixed using class F FA, GGBS and HMNS as a combined binder. The optimal combination of FA, GGBS and HMNS was determined based on the compressive strengths obtained from the GP pastes mixed with various different replacements of FA with GGBS and/or HMNS. The mechanical properties (compressive strength and splitting tensile strength) of the GP concrete mixed using the optimal combination of FA, GGBS, HMNS were tested at 7, 14 and 28 days and also compared with those of GP concrete without GGBS and HMNS. Microstructure analyses were carried out using SEM, XRD, FTIR to examine the difference in the material organization and morphological structure between the GP concrete specimens with and without GGBS and HMNS addition.

2. Experimental programme

2.1 Materials

The materials used for casting GP concrete specimens were aluminosilicate materials (class F FA, GGBS and HMNS), aggregate, and alkaline activators.

Class F FA, obtained from Manjung power plant at Perak in Malaysia, was used as the main binder material in the present experimental study. The average particle size of the FA is about 18 μm. The specific surface area of the FA is around 1.29 m^2/g. GGBS was obtained from the steel plant at Penang in Malaysia. The average particle size of the GGBS is about 138 μm. The specific surface area of the GGBS is around 0.106 m^2/g. HMNS was obtained from the steel plant in Shaanxi Province, China. The average particle size of the HMNS is about 280 μm. The specific surface area of the HMNS is around 0.0536 m^2/g. Fig.1 shows the particle size distributions of the FA, GGBS and HMNS. The chemical compositions of the FA, GGBS and HMNS are given in Table 1, which were determined by using x-ray fluorescence analysis.

River sand of sizes not exceeding 5 mm and gravel of sizes ranging between 5 mm and 19 mm were used as the fine and coarse aggregates, respectively. The density is 1204 kg/m^3 for the coarse aggregate and 1640 kg/m^3 for the sand. In the present experimental tests, the mass ratio of the sand-to-gravel was kept at 3:7 for all specimens, which is similar to that used in normal PC concrete. The gravel was saturated in water for about 2 hours, then left to dry at a room temperature of 25±2°C and a relative humidity of 85-90% for another 1 hour until the water film on the surface visibly vanished, before it was mixed with binders and alkaline activators. This was to ensure that the gravel would not over absorb the activator solution when they were mixed together.

The alkaline activators used in the present experimental study were sodium silicate (Na_2SiO_3) and sodium hydroxide (NaOH). The sodium silicate solution was obtained from South Pacific Chemicals Industries (SPCI) Ltd in Malaysia, with the chemical composition of Na_2O=14.7%, SiO_2=29.8%, and water 55.5% by mass. The sodium hydroxide solution was prepared in the laboratory by dissolving sodium hydroxide pellets in water. To prepare the sodium hydroxide

solution with the concentration of 12M, 480 grams of sodium hydroxide pellets supplied from Formosa Plastic Corporation, Taiwan were dissolved in 1 litre of distilled water. After cooling for 24 hours at room temperature, the sodium hydroxide solution was then mixed with the sodium silicate solution. The mass ratio of sodium-silicate to sodium-hydroxide solution was 2.5, which was previously used for producing FA based geopolymer concrete [29].

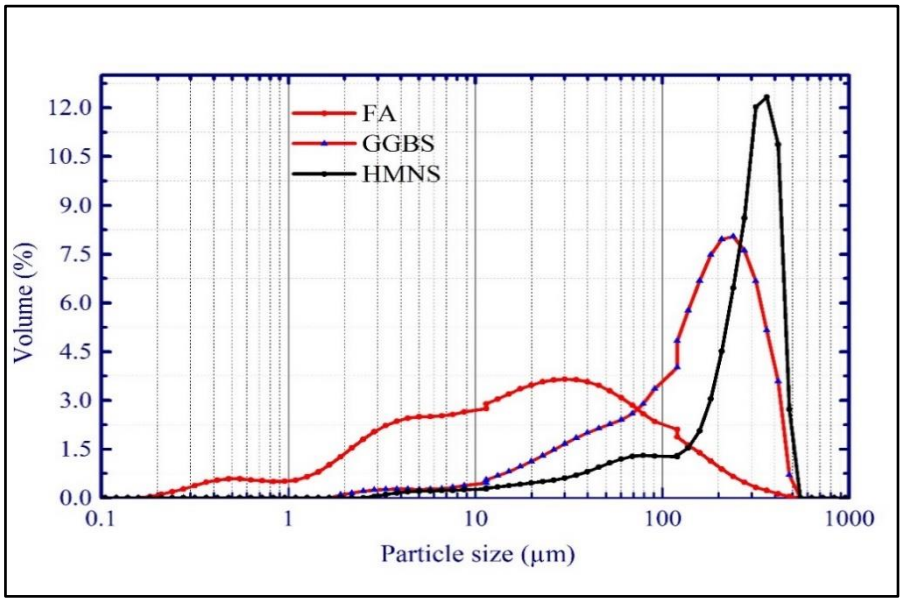

Fig. 1. Particle size distributions of FA, GGBS and HMNS.

Table 1.Chemical compositions of FA, GGBS and HMNS.

Compositions	Class F FA	GGBS	HMNS
SiO_2	55.7	28.2	43.22
Al_2O_3	27.8	9.73	4.35
Fe_2O_3	7.27	0.98	10.34
CaO	4.10	52.69	3.45
TiO_2	2.29	1.01	0.1
SO_3	0.27	1.46	0.28
K_2O	1.55	1.22	0.18
MgO	-	2.9	26.15
MnO	-	0.74	0.89
P_2O_5	-	-	0.05
Na_2O	-	-	0.23
Cr_2O_3	-	-	1.01
LOI	3.04	3.76	0.3

Others	1.018	1.05	9.4

2.2 Mix proportions of GP paste and GP concrete

Two types of GP pastes were mixed and tested. One is the GP pastes in which the binder consists of FA and GGBS. The other is the GP pastes in which the binder consists of FA, GGBS and HMNS. In both types of mixes, the binder-to-liquid (alkaline solution) ratio was kept at 2.0, which was suggested based on previous experimental results [29].

In the FA-GGBS based GP pastes, GGBS contents with 5%, 10%, 20%, 30% and 40% of the binder were selected. Nine specimens of 50 mm x 50 mm x 50 mm cube for each selected GGBS content were cast. Hence, there were a total of 5x9 = 45 cubic specimens that were cast. The compressive strength tests were carried out on these specimens at 7, 14, and 28 days, respectively; and at each time three specimens were tested repeatedly for each selected GGBS content specimens. The purpose of the tests was to find out the best FA-to-GGBS ratio, which gives the largest compressive strength.

In the FA-GGBS-HMNS based GP pastes, GGBS content was fixed at the optimum portion of 20%, which was determined based on the largest compressive strength of the FA-GGBS based GP pastes, whereas HMNS was used to partially replace FA with the replacement of 5%, 10%, 15% and 20%. Six specimens of 50 mm x 50 mm x 50 mm cube for each selected HMNS content were

cast. Hence, there were a total of 4x6 = 24 cubic specimens that were cast. The compressive strength tests were carried out on these specimens at 7 and 14 days, respectively; and at each time three specimens were tested repeatedly for each selected HMNS content specimens. The purpose of the tests was to find out the best FA-to-HMNS ratio, which gives the largest compressive strength.

The contents determined from the GP pastes for GGBS and HMNS were used to cast the FA-GGBS-HMNS based GP concrete. Two types of GP concrete specimens were cast. One is the cubic specimens of 100 mm x 100 mm x100 mm, used for conducting compressive strength tests at 7, 14, 28 and 90 days (3x4=12 specimens); each time with three repeat tests. The other is the cylindrical specimens of diameter 75 mm and length 150 mm, used for conducting splitting tensile strength tests also at 7, 14, 28, and 90 days (3x4=12 specimens); each time with three repeat tests. All of the FA-GGBS-HMNS based GP concrete specimens have the same mix proportion with the binder-to-liquid ratio being 2:1 and the binder-to-aggregate ratio being 3:7. Table 2 shows the details of the mix design proportions for GP paste and GP concrete.

Table 2. Mixture proportions of GP paste and GP concrete

Materials	GP Paste	GP concrete	
	Cubic specimens	Cubic specimen	Cylindrical specimen
Coarse aggregates, kg/m^3	-	1176	779
Fine aggregates, kg/m^3	-	504	333.7
Class F FA, kg/m^3	420	336	222.6
GGBS, kg/m^3	120	96	63.6
HMNS, kg/m^3	60	48	31.8
Na_2SiO_3 solution, kg/m^3	214.28	171.43	113.6
NaOH solution (12M), kg/m^3	85.71	68.6	45.5
Na_2SiO_3/NaOH ratio	2.5		
Solid/alkaline activator ratio	2.0		

After they were cast, the GP paste and GP concrete specimens were covered using plastic film/sheet for 24 hours. Then they were demoulded and cured in laboratory conditions at room temperature of 25±2°C with a relative humidity of 85-90% condition before the specimens were tested.

2.3 Testing of GP paste and GP concrete

Fresh properties of GP paste and GP concrete were determined using setting time tests by using Vicat apparatus as shown in Fig.2 and workability tests using the slump test as shown in Fig.3, respectively. The compressive strength tests and splitting tensile strength tests were performed using a universal testing machine, under a load control regime with a loading rate of 0.3 kN/s for the compressive strength tests and a constant load rate of 1.0 kN/min for the tensile strength tests in accordance with the ASTM C496 standard [36], as shown in Fig.4. All tests were carried out in triplicate and average values were obtained and used as the results.

A scanning electron microscope (SEM) Hitachi S-4800 equipped with an energy dispersive x-ray (EDX) analyser (Brucker 5030) with an accelerating voltage of 10 kV, was used for morphological analysis evaluated under a low-vacuum mode and also for chemical analysis of the powder samples taken from the specimens. The samples used for SEM analysis were embedded in an epoxy resin and polished. To prepare the polished samples, a low speed diamond saw was used to slice a thick slices of 1~1.5 mm thickness, impregnated with low viscosity resin, then polished using SiC grinding papers of 240 grit. Final polishing step was conducted by utilizing polishing cloths and water based diamond suspension of 1 and 6 µm. The resulting surface was metallised with gold before the analysis in back-scattering mode.

An X-Ray Diffraction (XRD) was used to characterize and identify diverse crystalline and amorphous phases of the designed GP paste. XRD-6000 SHIMADZU X-Ray Diffractometer with Cu-Kα radiation generated under 40 mA and 44kv at room temperature, was used to examine four selected specimens. The XRD analysis was performed at a scanning angle 2θ ranged between 10 and 70°. The analysis was run for 44 seconds per 2θ step. Then, the diffraction patterns were analysed using a software called “X'Pert HighScore Plus” to identify and auto-match the peaks.

Fourier infrared spectroscopy analysis (FTIR) was carried out to identify the different function groups of the produced GP paste by using a Perkin Elmer Spectrometer 2000 in transmittance mode with a frequency ranged between 4000 cm^{-1} and 650 cm^{-1} at 4 cm^{-1} resolution. The specimens were evaluated by applying Potassium Bromide (KBr) pellets methodology.

Fig. 2.Vicat apparatus

Fig. 3.Slump test

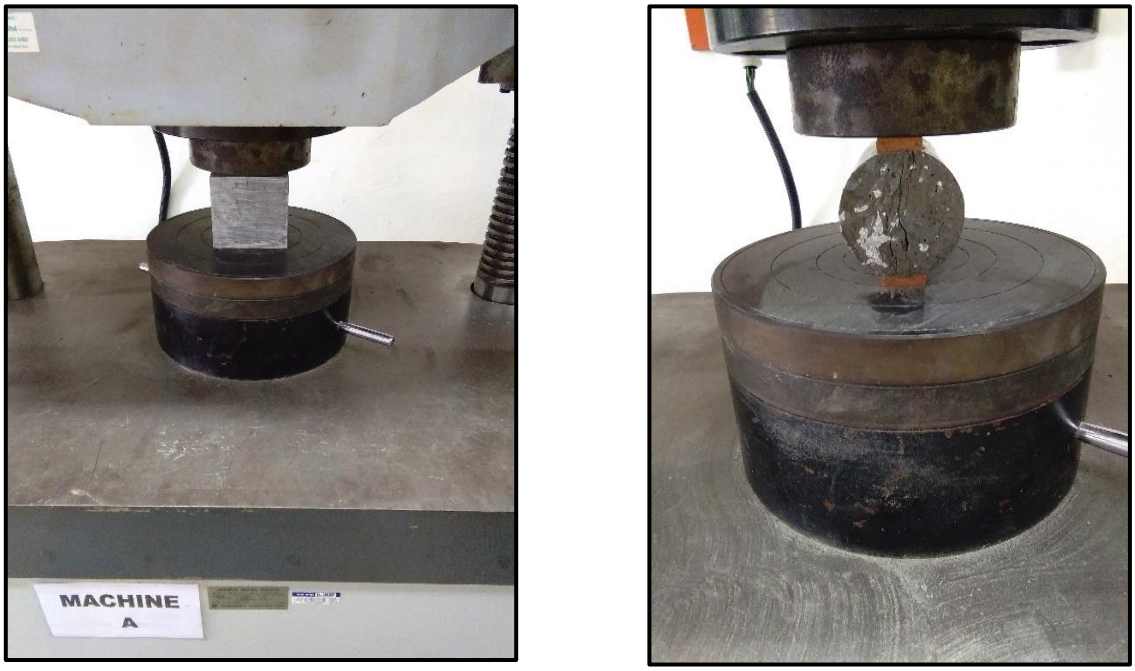

(a) (b)

Fig. 4. (a) Compressive strength and (b) Splitting tensile strength tests.

3. Results and discussion

3.1 GP paste

Fig.5 shows the compressive strengths of the FA-based GP paste specimens with different GGBS replacements, tested at ages of 7, 14 and 28 days, respectively. It can be seen from the figure that, for GGBS replacement less than 30%, the compressive strength increases with the time. However, when GGBS replacement reaches 30% the compressive strength increases from 7 days to 14 days, but after 14 days it decreases with time. The latter could be due to the excess of Ca content sourced from the GGBS in the mixture as inactive and unreacted constituents, which affects the condensation process and inhibits the continuity of the formation of geopolymer gels, and subsequently it causes the reduction of both setting time and compressive strength. When GGBS replacement reaches 40% the compressive strength was found to decrease with time, which is opposite to the strength development found in the specimens with GGBS replacement less than

30%. This indicates that too much GGBS has a negative effect on strength development. Also, it can be observed from the figure that the compressive strength of the FA-based GP paste increases initially and then reduces with the increased GGBS replacement, the case of which is similar to that of 30% replacement. The maximum compressive strengths at age 7, 14 and 28 days were found to be 38.5, 45.6 and 76.6 MPa, respectively, which occurred at the GGBS replacement of 20%. Comparing the compressive strength of FA-based GP paste without GGBS (73.86 MPa) cured at the same conditions, the use of 20% GGBS replacement can increase the compressive strength by about 3.7%. A similar result was also found by Nath and Sarker [30], who reported that the FA-based paste had a strength increase when FA was partially replaced with GGBS. However, they found the maximum compressive strength was at the 30% GGBS replacement, which is slightly different from what we found here. The reason for this could be due to the different sources used for taking the FA and GGBS.

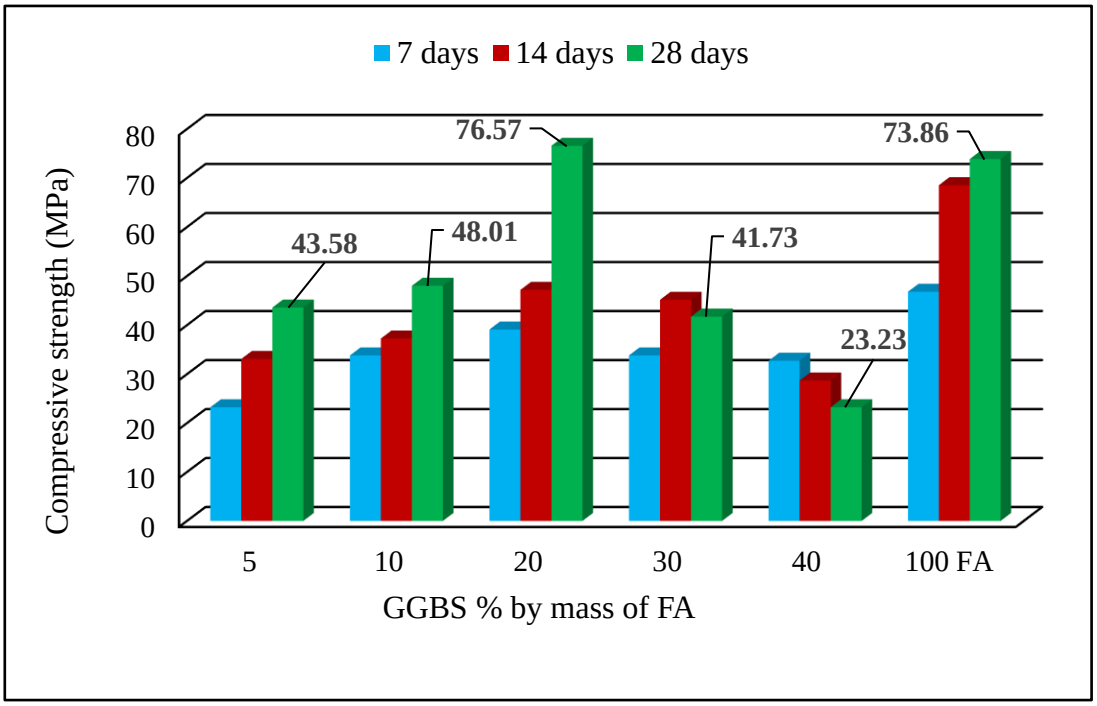

Fig. 5. The compressive strength of FA-based paste with different GGBS replacement.

Fig.6 shows the compressive strengths of the FA-GGBS (20%)-based GP paste specimens with different HMNS replacements to FA, tested at ages of 7 and 14 days, respectively. It can be seen from the figure that, for all tested specimens the compressive strength at 14 days is higher than that at 7 days, indicating that the HMNS has no negative effect on the strength development. Also,

it can be observed from the figure that the highest compressive strength is when 10% HMNS replacement to FA was used, which gave the 14-day compressive strength of 60.82 MPa. Comparing the 14 days compressive strength of the FA(80%)-GGBS(20%) based GP paste without HMNS (47.2 MPa), the use of 10% HMNS replacement to FA can increase the compressive strength by about 29%, which is highly significant. This improvement in strength is mainly due to the high contents of magnesium in the mixture, which plays a similar role to the calcium and produces a new hydrate gel called hydrotalcite-like phase or magnesium-bearing silicate hydrates (M-S-H or C-M-S-H) [20,24]. A report produced by Zhang et al. [20] showed that the use of HMNS in FA-based GP concrete has a positive effect on the compressive strength of the mixture when its replacement is not over 60%. Otherwise, it will have a negative effect on the compressive strength.

It is believed that the combined use of class F FA, GGBS and HMNS mitigates the porosity of the matrix, by reducing its dehydration which leads to mass loss of the produced GP material. The use of 100 % of class F FA in the production of geopolymers mainly produces a major A-S-H gel phase, which is generally high porous as indicated in many previous research [24,32]. The combined use of FA and GGBS in GP concrete has been reported in literature and it has been demonstrated that the blending of these two materials in geopolymers can result in the formation of binary A-S-H and C-A-S-H gel phases, which improve the mechanical properties of the GP, and also control its fresh properties due to the influence of GGBS content. A previous study by Yang et al. [31] showed that the C-A-S-H gel formed due to the incorporation of GGBS was vulnerable when exposed to a high temperature and showed a considerable degradation. They also found that when HMNS was blended with GGBS it produces a high N-A(M)-S-H gel in the system.

Based on the results of the compressive strength of GP paste specimens described above it is concluded that the mixture of 70% FA, 20% GGBS and 10% HMNS provides the highest compressive strength. This proportion thus was to be used for the casting of concrete specimens.

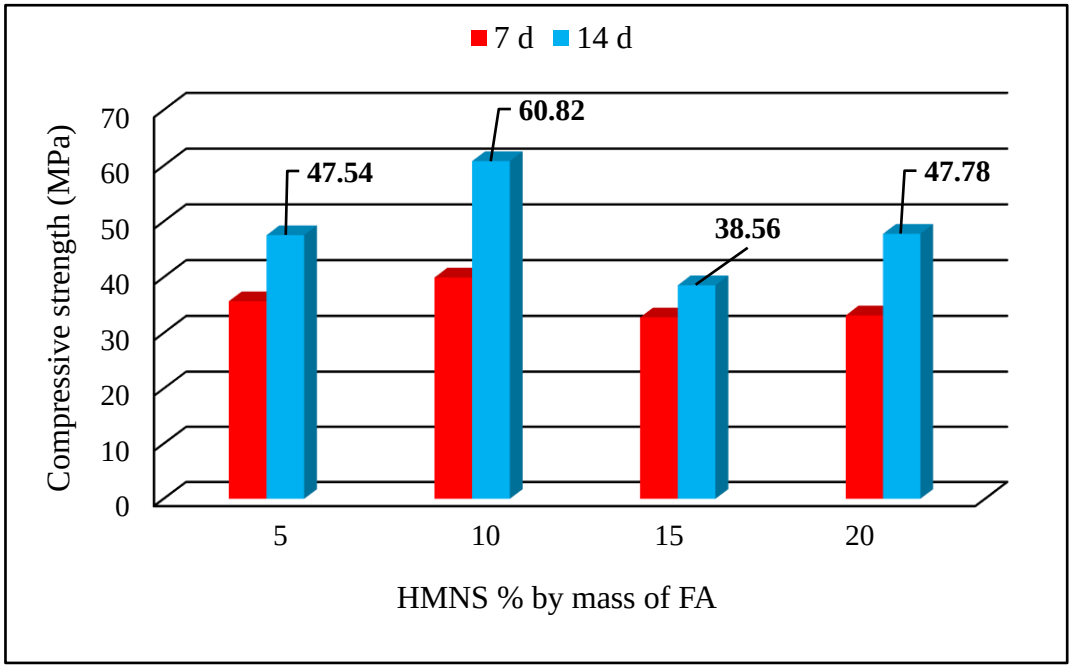

Fig. 6. The compressive strength of FA-GGBS based paste with different HMNS replacements (GGBS replacement was kept as 20%).

3.2 GP concrete

The GP concrete cubic and cylindrical specimens were mixed using the proportion as shown in Table 2. The workability of the GP concrete was examined by using the setting time test, which was performed on the fresh GP paste, whereas, the slump test was implemented on the fresh GP concrete as shown in Figs.7a and 7b, respectively. The setting time was obtained directly using the Vicat apparatus. The initial setting time started when an activator solution was added to the dry mixture until the time when the paste began to lose its elasticity, which corresponds to 310 min as shown in Fig.7a. The final setting time elapsed from the moment when the paste completely lost its elasticity, which corresponds to 1490 min as shown in Fig.7a. Both the initial setting time and final setting time seem reasonable for concrete although the final setting time was found to be slightly longer than the normal final setting time for traditional concrete. This could be due to the continuity of geopolymerization reactions taking place in concrete because of the high amorphous phase of HMNS, which needs more time to be reacted and to formulate (M-S-H or C-M-S-H) gels.

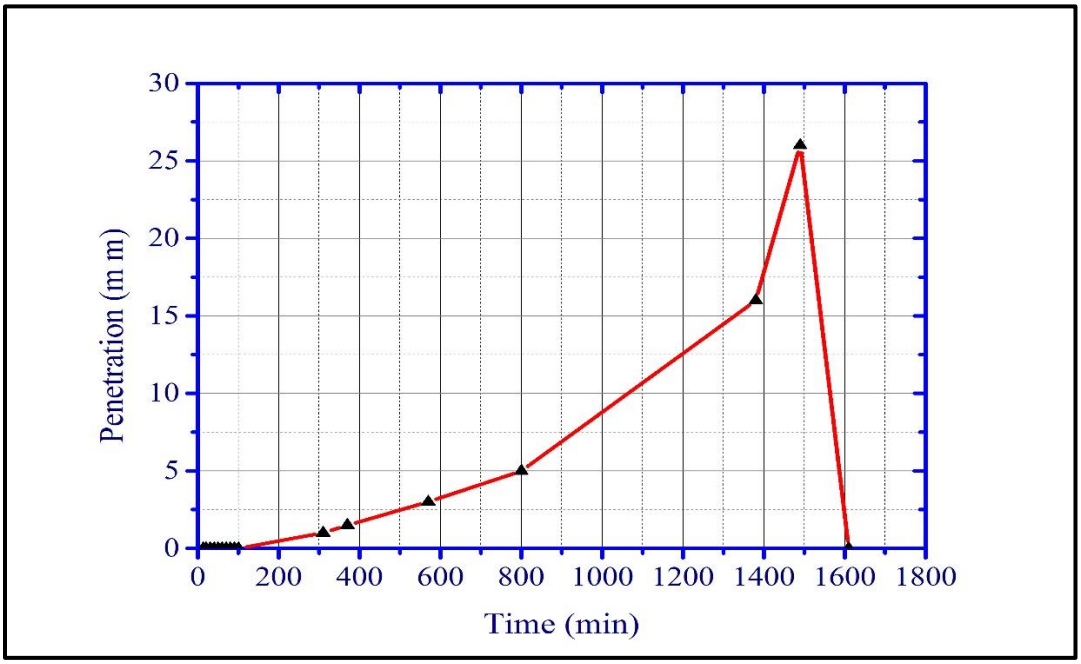

(a)

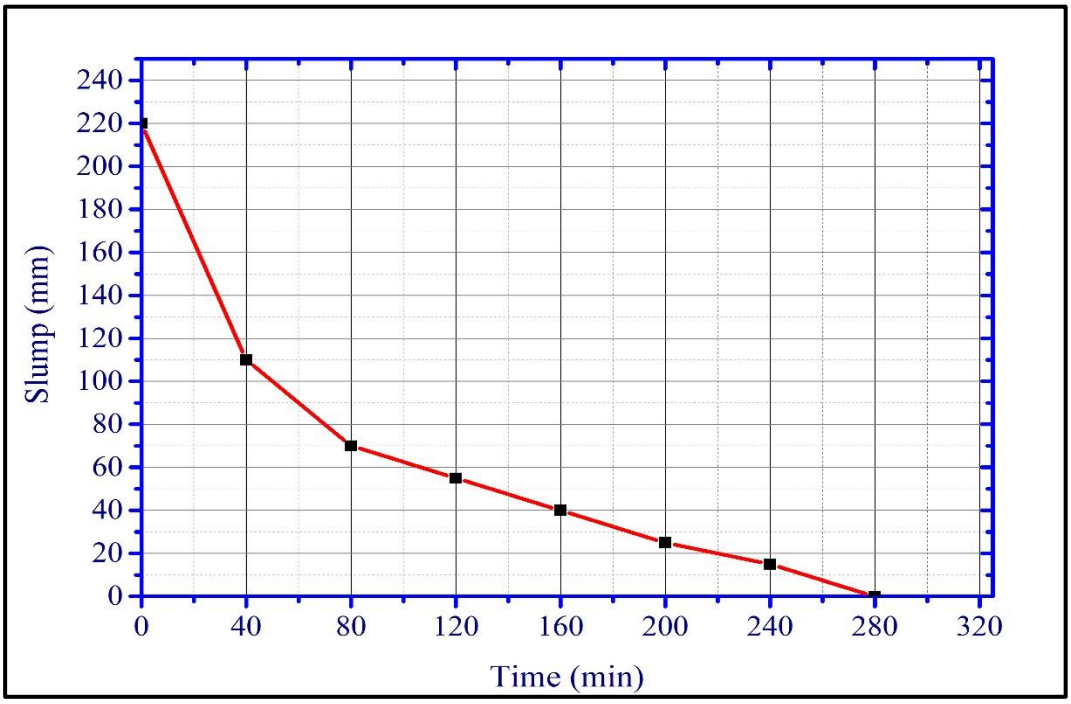

(b)

Fig. 7. (a) Setting time of GP paste and (b) slump test of GP concrete.

The slump test result of the fresh GP concrete is shown in Fig.7b. The procedure was repeated several times, which demonstrated the good workability of the designed GP concrete. Note that, the workability of a concrete is controlled not only by the binders but also by the aggregate and the alkaline activators. It is believed that the mixed sizes and proportion of FA, GGBS, HMNS

and aggregate played a significant role in the improvement of workability, which leads to creating what is called inter-particles dynamism in the system, which make the released molecule of water easily penetrate between particles during geopolymerization.

The compressive strengths of the designed GP concrete at 7, 14, 28 and 90 days are shown in Fig.8a-(A). It can be seen from the figure that the compressive strength increases from 27.17 MPa at 7 days to 55.60 MPa at 28 days, and then reduces a little from 55.60 MPa at 28 days to 48.14 MPa at 90 days, indicating that the strength was fully developed during the first 28 days curing, whereas the afterwards strength reduction was about 14%. This reduction in compressive strength after 28 days is mainly due to the continuity of geopolymerization reaction with FA, which leads to the formation of more porous A-S-H gel compared to the C-S-H gel formed due to the presence of GGBS [32]. For the purpose of comparison, the compressive strengths reported by other researchers for the FA-based GP concrete with similar mixes and curing conditions are also superimposed in Fig.8a indicated as letters B, C and D [33-35]. The figure shows that, in overall, the designed GP concrete based on the test results of GP pastes has about 10% higher compressive strength than others. The improvement in strength of the GP concrete is partly because of the rapid formation of C-S-H and A-S-H gels during its geopolymerization as is confirmed by SEM/EDX analysis in Fig.10 to be discussed lately, and partly because of the different particle size distributions of FA, GGBS and HMNS, which makes the mixed concrete less porous.

The splitting tensile strengths of the designed GP concrete at 7, 14, 28 and 90 days are shown in Fig.8b, which were obtained experimentally by following ASTM standard C496 [36]. It can be seen from the figure that the splitting tensile strength increases from 2.89 MPa at 7 days to 4.57 MPa at 28 days, and then reduces a little from 4.57 MPa at 28 days to 4.12 MPa at 90 days. The variation of the splitting tensile strength with age is very similar to that of the compressive strength with age, indicating that there might be a good correlation between the compressive strength and splitting tensile strength. Similar to the compressive strength, the 28 days splitting tensile strength of the designed GP concrete presented in this study is also 10% higher than that of the similar GP concrete reported in the literature by Sofi et al. [34], as shown in Fig.8b-E, where the GP concrete was made at room temperature and relative humidity >80%.

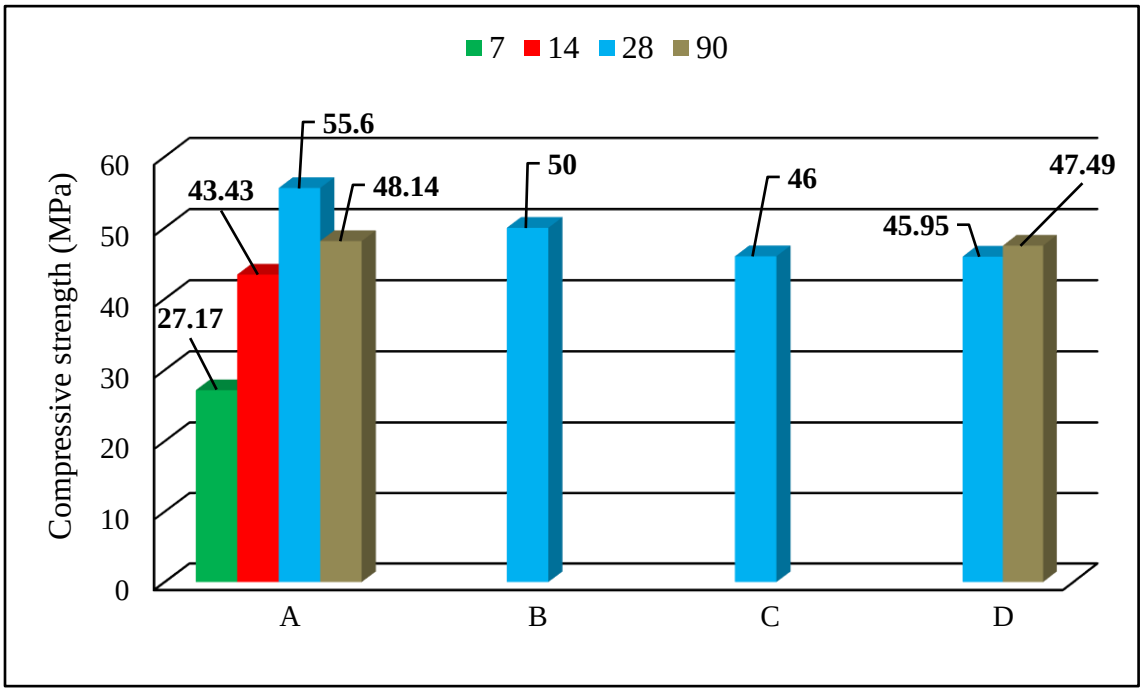

(a)

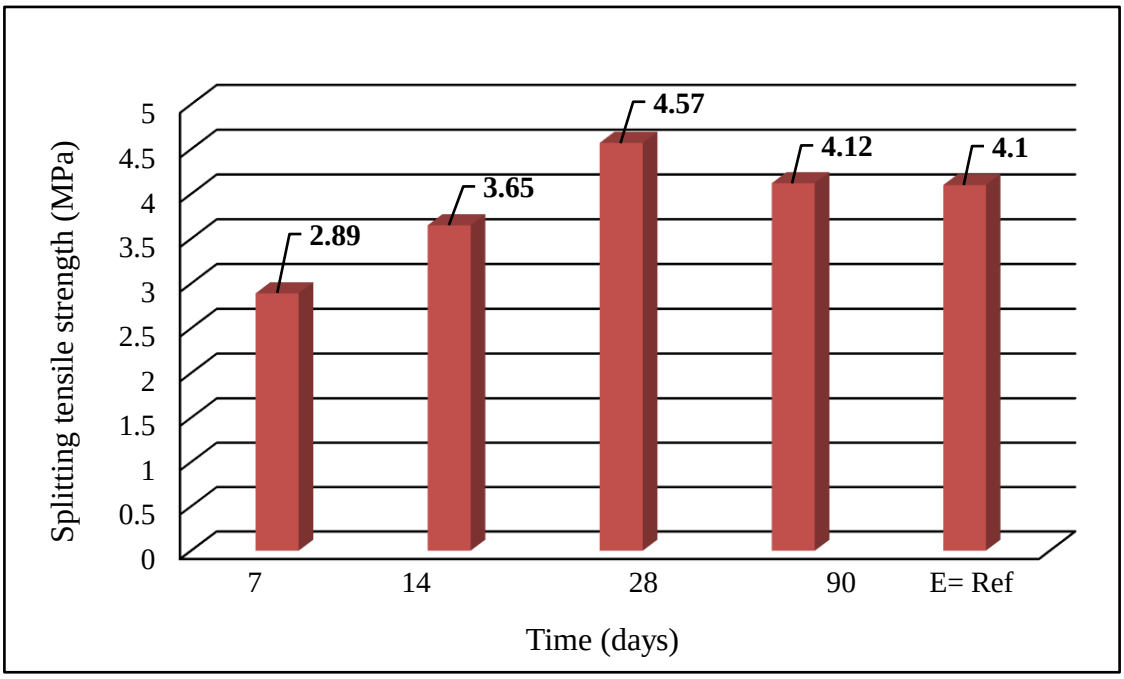

(b)

Fig. 8. (a) Compressive strength and (b) splitting tensile strength of GP concrete. *Mix B and E were prepared using class F FA and GGBS and activator solution consists of sodium carbonate (Na_2CO_3), sodium silicate (Na_2SiO_3), and sodium hydroxide (NaOH). Mix C was prepared using*

low calcium FA blended with small percentage of additive of GGBS, OPC, or hydrate lime, the alkaline activator was a mixture of sodium hydroxide and sodium silicate. Mix D was prepared using low calcium FA activated with sodium hydroxide and sodium silicate solution.

3.3 SEM images

The SEM images of the FA-based GP pastes with varying GGBS and HMNS replacements, are shown in Fig.9. It is evident from these images that the paste with 70% FA, 20% GGBS and 10% HMNS exhibits a denser microstructure and almost fully reacted matrix with some unreacted cenosphere and plerospheres FA particles. It was reported that the unreacted particles do not act as filler in the mixture, but lead to an increase in the strength of the matrix with age [37].

The images shown in Figs.9b and 9c demonstrate the geopolymerization products and show the presence of C-S-H and A-S-H gels, which were mainly created from the activation of the 20% of GGBS, which in turn interacts with the FA, as can be observed on the EDX images [38, 40]. The high source of the calcium and alumina-silicate in the mixture led to the formation of calcium alumina-silicate hydrate gel (C-A-S-H). GGBS, therefore, sourced an additional amount of calcium and contributed to an additional binding product, which in turn affects the setting behaviour of geopolymer gel [30]. It is highly possible for the Mg^{2+} which is sourced from the HMNS to contribute in the formation of new gel phase as Na-Al(Mg)-Si-H gel, as evidenced by the EDX analysis [20]. The micro-cracks observed in some of the SEM features probably occurred during the mechanical tests, since the powders tested for SEM were taken from the specimens after the mechanical tests. Such micro-fissures could also be the result of multi-sequences of an internal stress occurred between particles during microstructural development [39]. The presence of shaped-needles on the fly ash particles as appeared in Fig.9a2, is probably due to the high concentration of the activator solution in the mixture. This unreacted alkali solution precipitated as micro-needle particles in the mix during geopolymerization process [41].

Fig.10 presents the EDX analysis associated with the morphological images (SEM). It shows that the selected area has major elements of silicon, aluminium, calcium, sodium and magnesium as illustrated in Table 3. The EDX results were in good agreement with the XRD results to be shown in next section, where some patterns, such as quartz remained due to the partial dissolution of the raw materials.

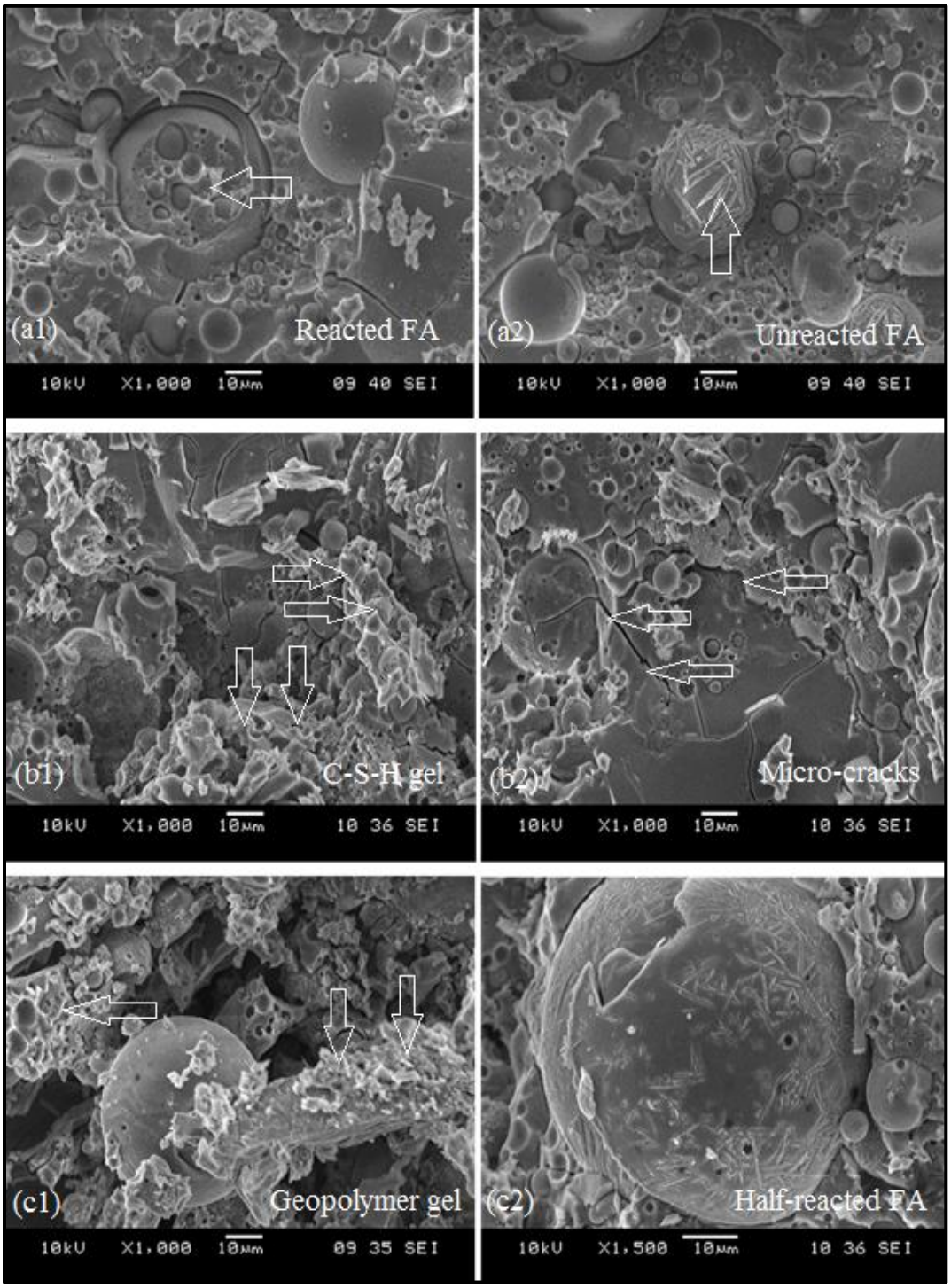

Fig. 9. SEM images of FA-based GP pastes.

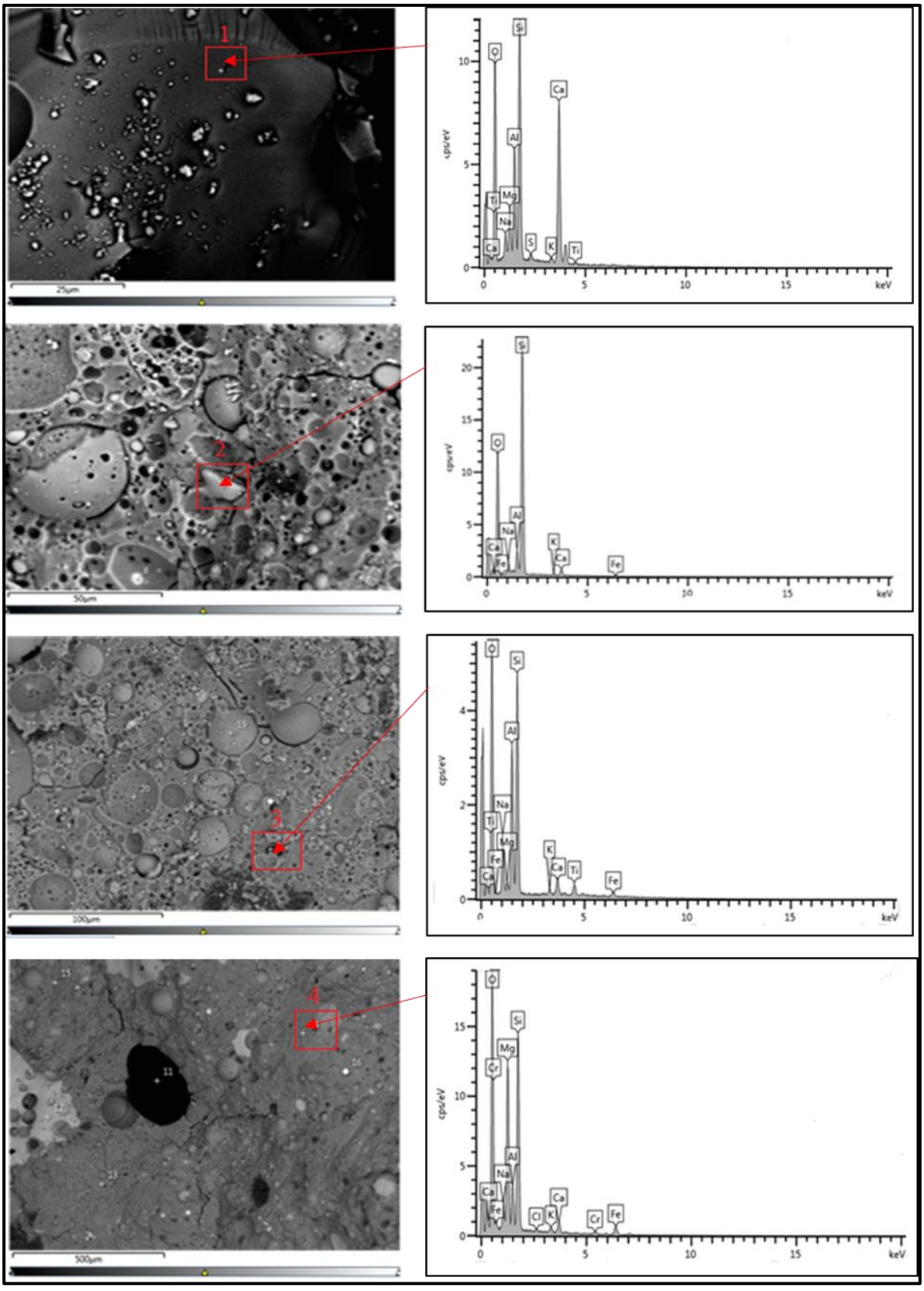
1
25µm
O
Si
Ca
Al
Mg
Ti
Na
S
K
Ca
Ti
cps/eV
keV
2
50µm
O
Si
Al
Na
K
Ca
Fe
cps/eV
keV
3
100µm
O
Si
Al
Na
Ti
Mg
Fe
K
Ca
Ti
Fe
cps/eV
keV
4
500µm
O
Si
Mg
Cr
Al
Na
Ca
Fe
Cl
K
Ca
Cr
Fe
cps/eV
keV

Fig. 10. SEM/EDX of selected areas from the produced GP matrix.

Table 3. Relevant element percent of the selected areas from Figure 10.

Element (Wt %)	Area 1	Area 2	Area 3	Area 4
Si	18.0	39.7	22.4	21.4
Al	8.1	3.7	13.8	4.9
Ca	24.5	2.1	3.2	2.2
Mg	3.8	-	0.9	16.5
Na	2.0	2.5	7.0	3.0

3.4 XRD analysis

The XRD patterns of FA-based GP paste cured at ambient temperature are shown in Fig.11. It can be seen from the pattern shown in Fig.11a that the main identified crystalline peak in FA was the quartz (SiO_2) with a high intensity at 2θ =27º, which is supported by the XRF results where 55.7% of SiO_2 was detected. Mullite ($Al_6O_{13}Si_2$) was another important peak detected in different ranges of 2θ (17º and 65º) [40]. Fig.11b shows that the main mineral elements found in GGBS were calcium carbonate ($CaCO_3$) and quartz (SiO_2) at 30º and 27º-50º, respectively. The XRD pattern shown in Fig.11c suggests that many crystalline phases were characterized in HMNS with a high peak of magnesium silicate ($MgSiO_3$) at 2θ=27º [24, 42], where albite (Na ($AlSi_3O_8$)) was stretched at 2θ=18º, 23º and 53º and nickel magnesium silicate ($Mg_{1.4}Ni_{0.6}O_4Si$) at 2θ=32º and 37º. Fig.11d shows the XRD patterns of the designed GP concrete. It is evident that magnesium vanadium molybdenium oxide ($Mg_{2.5}(VMo)O_8$) from HMNS is the main identified peak with a high intensity at 2θ=27º. It is also seen from the XRD result that new crystalline peaks appeared in the pattern, matched the calcium beryllium praseodymium oxide ($CaBePr_2O_5$), which has an orthorhombic crystallography and pnma space group. These new crystalline phases could be attributed to the presence of GGBS and HMNS, where their glassy phases were activated due to the high pH of the environment.

However, there is no formation of $Mg(OH)_2$ crystalline products detected in the binder, which could lead to an undesired expansion of the geopolymer structure [24]. In addition, it can be

observed from the XRD patterns of the GP paste that the source materials have influence on the geopolymerization in two ways: The first one is mainly related to the broad hump on the XRD patterns of the GP paste, which also appears between 15º and 40º in the XRD patterns of the FA and GGBS. The hump shown in the XRD pattern of the GP paste corresponds to the formation of a new amorphous hump and was identified as the geopolymeric gel. The second one is related to the decrease in the intensity of the crystalline peaks. This reveals a partial dissolution of the crystalline phases of the precursor materials, such as the quartz (SiO_2) from FA and the calcium carbonate ($CaCO_3$) from GGBS. It was reported that the decrease of the intensity of the crystalline phases could be due to the presence of sodium silicate [45].

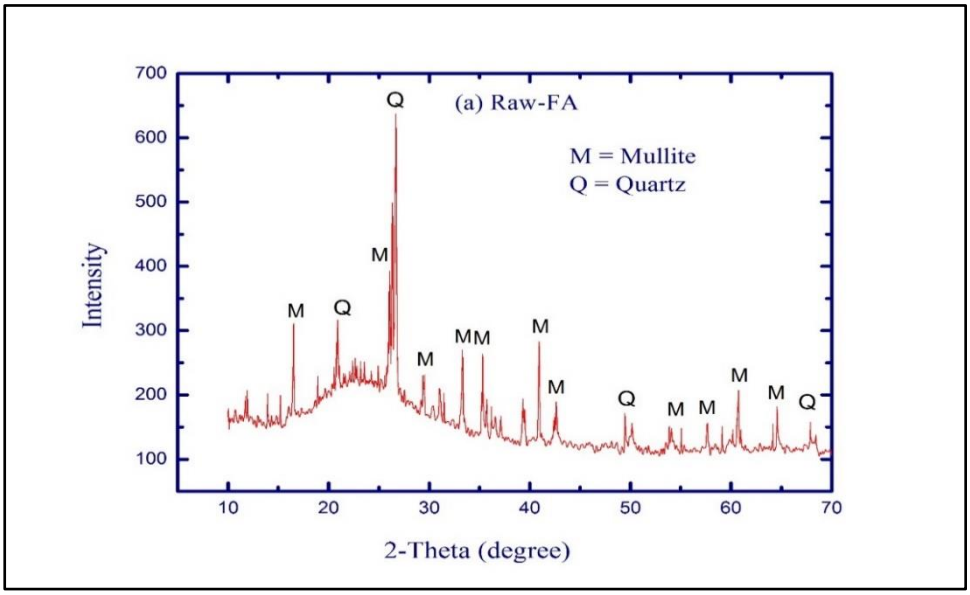

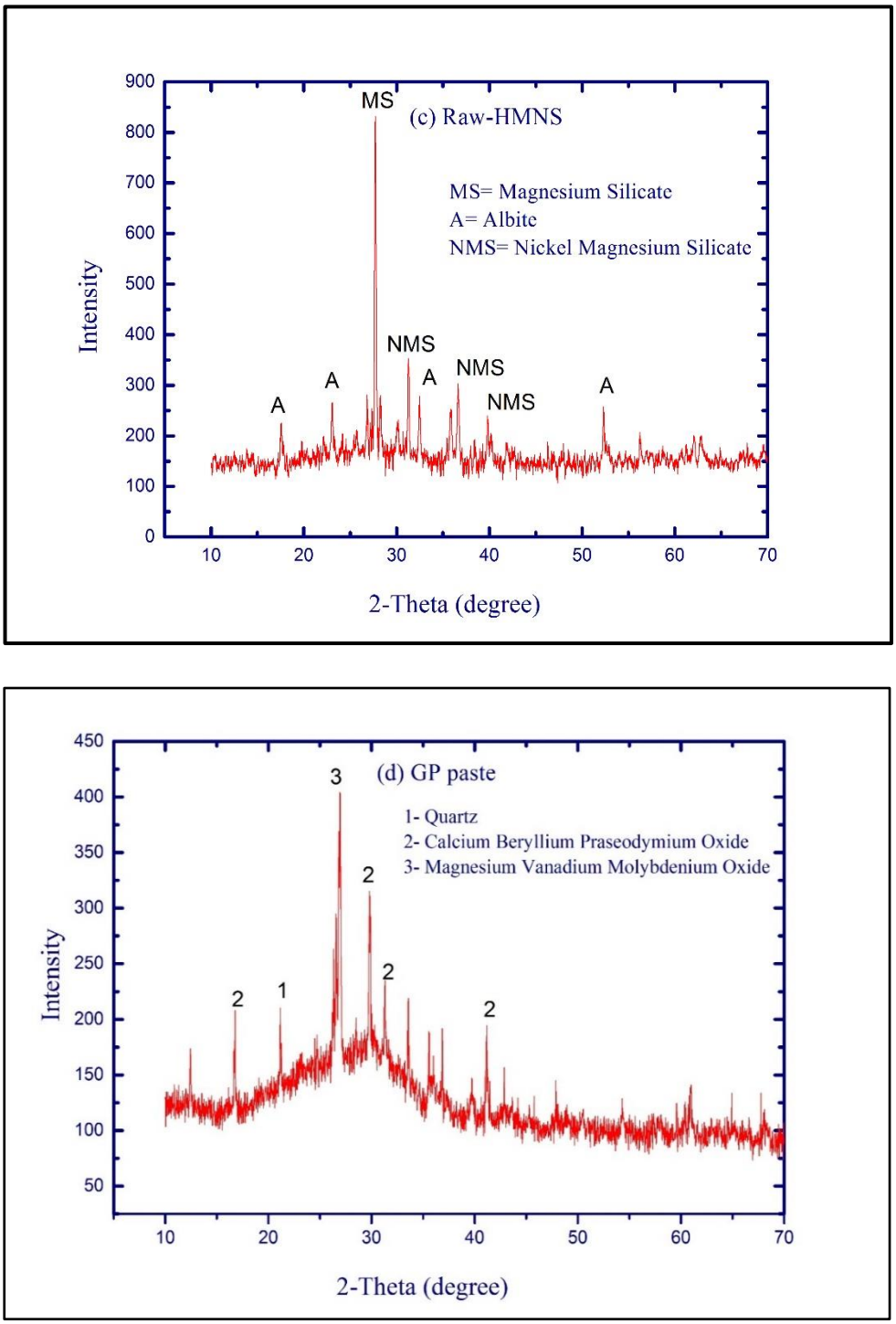

Fig. 11. X-ray diffractograms of the used raw materials and the manufactured GP paste.

3.5 FTIR analysis

The FTIR spectra of the GP concrete cured at room temperature at age 28 days are shown in Fig.12. The difference in the absorption frequency of the GP products is characterized by various bands and function groups formed during geopolymerization. The bands at ~ 3300-3600 cm^{1-} revealed that there is stretching vibration of O-H bending [43, 44, 45]. While the bands at 2000-2200 cm^{-1} could correspond to the stretching vibration of the functional group of Na_2CO_3, K_2CO_3 or sodium phosphate, formed by the activator solution and the binder material during the geopolymerization process. Typically, if there is an excess of sodium ions due to the high concentration of alkali solution, a portion of it is transferred to the surface where it carbonates with the carbon dioxides from the atmosphere [46, 47]. The stretching vibration frequency at ~ 2500 cm^{-1} can be C=O. The bands at ~ 1670 cm^{-1} present the H-O-H group. The frequencies of CO_3^{2-} with stretching vibrations of C-O groups were characterized at the peaks ~1470 cm^{-1} [48]. The broad band at around 940-1005 cm^{-1} can be ascribed to the asymmetric and symmetric stretching vibrations of Si-O-Si and Al-O-Si, which are formed during the dissolution of SiO_4 tetrahedra, generally the bands centred in these regions correspond to the C-S-H gel [49, 50]. However, the bands Si-O and Al-O were stretched at ~ 850 cm^{-1} and the stretching vibration of $–CO_3$ was counted at 875 cm^{-1} [45, 51].

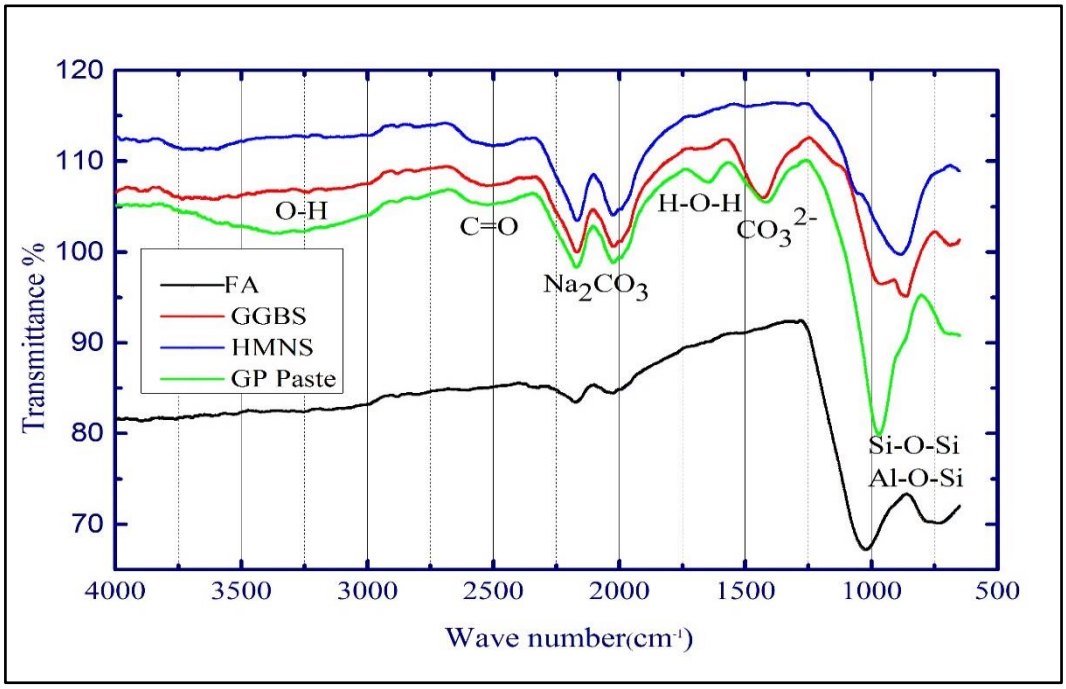

Fig. 12. The FTIR spectra of raw materials and GP paste.

This study shows a good improvement of the mechanical and microstructure properties of the GP concrete mixed using FA, GGBS and HMNS. The combination of those three materials led to the formation of ternary gel phases, due to the occurring of different chemical reactions in the mixture with the presence of the alkali activator solution. It was also demonstrated that the M-S-H or C-M-S-H gel sourced from the HMNS is denser and morphological less porous when compared with the A-S-H and C-S-H gels formed from FA and GGBS. It is clear that the incorporation of HMNS with class F FA and GGBS introduces a significant improvement on the engineering properties. The sourced Mg^{++} cations from HMNS improve the geopolymerization of geopolymeric system. The chemical nature of the magnesium allows the Mg^{++} cations to form a strong intermolecular bonding with other cations such as Si^{+4} and Al^{+3} through sharing of oxygen atoms as schematised in Fig.13. The proposed model shown in Fig.13 is fundamentally similar to that proposed by Davidovits [52]. Further, the presence of Mg^{++} in the geopolymeric chain provides chemical stability or what is called interatomic-bonding in the matrix, due to the formation of different chain-links such as Si-O-Mg, Si-O-Al, Ca-O-Si and Si-O-Si. Therefore, it is believed that such intermolecular forces created in the system can be a reasonable explanation for the improvement of the GP properties.

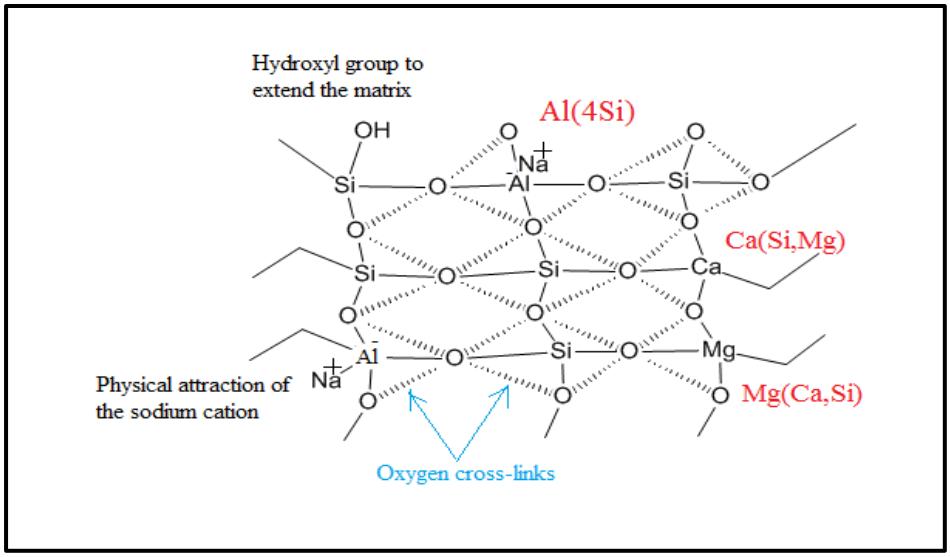

Fig.13.Proposed model of the ternary A-S-H, Ca-S-H, and C-M-S-H gel phases.

4. Conclusions

The mechanical and microstructural properties of FA-GGBS-HMNS-based geopolymer paste and concrete were investigated experimentally in this paper. The effects of using GGBS and HNMS as a partial replacement of FA on the compressive strength and splitting tensile strength of the mixed GP paste and GP concrete were examined. It was found that the GP paste and GP concrete mixed with 70% FA, 20% GGBS and 10% HNMS exhibited higher mechanical properties, with a compressive strength of 55.6 MPa and a splitting tensile strength of 4.57 MPa. The morphological and microstructural analysis showed that there are additional formations of crystalline phases. These are derived from different minerals such as Mg, Ca, Si, Al and Na. The XRD results showed the formation of C-S-H, C-A-S-H and other new gel phases such as magnesium vanadium molybdenium oxide and calcium beryllium praseodymium oxide, which are mainly sourced from GGBS and HMNS as main sources of calcium and magnesium respectively.

The SEM analysis showed that the manufactured GP concrete is highly compacted, with a dense matrix and fewer pores. The EDX analysis associated with SEM images and FTIR results confirm that a partial replacement of FA with GGBS and HMNS enhances the mechanical properties of the produced GPC. This is mainly due to the formation of new crystalline phases as a result of the incorporation of Ca^{++} and Mg^{++} into the geopolymer gel. Therefore, the combination of FA, GGBS and HMNS results in the formation of ternary gels C-S-H, A-S-H and Na-Al(Mg)-Si-H, which leads to the improvement of the mechanical properties of the produced GP products. This study highlights the future research and the development of geopolymer concrete technology, by focusing on two potential solutions. First, it can use industrial by-products and decrease the amount of harmful waste materials. Second, it can be used as new alternative sources of cementitious material, which have a lower greenhouse footprint than the conventional concrete.

Acknowledgement - The authors would like to acknowledge the support received from the European Commission Research Executive Agency via a Marie Skłodowska - Curie Research and Innovation Staff Exchange project (689857-PRIGeoC-RISE-2015).

References

[1] ICE (2011): Building a Sustainable Future - ICE low carbon infrastructure trajectory – 2050. Institution of Civil Engineers, One Great George Street, Westminster, London SW1P 3AA.

[2] V.M. Malhotra, Introduction: sustainable development and concrete technology, Concr Int. 24(7) (2002) 22.

[3] M.S. Imbabi, C. Carrigan, S. McKenna, Trends and developments in green cement and concrete technology. International Journal of Sustainable Built Environment. 1 (2012) 194-216.

[4] E. Gartner, Industrially interesting approaches to 'low-CO2' cement, Cem Concr Res. 34(9) (2004) 1489–1498.

[5] S.O. Ogbeide, Developing an optimization model for CO2 reduction in cement production process, J Eng Sci Technol Rev. 3(1) (2012) 85–88.

[6] R. Snellings, G. Mertens, J. Elsen, Supplementary cementitious materials, Reviews in Mineralogy and Geochemistry. 74(1) (2012) 211-278.

[7] K.H. Yang, J.K. Song, K.I. Song, Assessment of CO2 reduction of alkali-activated concrete, J Clean Prod. 39 (2013) 265–272.

[8] J. Davidovits, Geopolymers: inorganic polymeric new materials, J Therm Anal, 37 (1991) 1633-56.

[9] A. Karthik, K. Sudalaimani, C.T. Vijaya Kumar, Investigation on mechanical properties of fly ash-ground granulated blast furnace slag based self-curing bio-geopolymer concrete, Construction and Building Materials. 149 (2017) 338-349.

[10] R. Anuradha, R. Balathirumal, P.N. John, Optimization of molarity on workable self-compacting geopolymer concrete and strength study on SCGC by replacing fly ash with silica fume and GGBFS, Int. J. Adv. Struct. Geotech. Eng. 3(1) (2014) 11-18.

[11] S. Andini, R. Cioffi, F. Colangelo, T. Grieco, F. Montagnaro, L. Santoro, Coal fly ash as raw material for the manufacture of geopolymer-based products, Waste Manag. 28 (2008) 416-423.

[12] ASTM C618, Standard specification for coal fly ash and raw or calcined natural pozzolan for use in concrete. American society for testing and materials. West Conshohocken, PA, USA: ASTM International; 2003.

[13] A. Palomo, A. Fernández-Jiménez, G. Kovalchuk, L.M. Ordoñez, M.C. Naranjo, OPC-fly ash cementitious systems: study of gel binders produced during alkaline hydration, Mater Sci. 42 (2007) 2958-2966.

[14] N. Bouzoubaâ, M.H. Zhang, V.M. Malhotra, Mechanical properties and durability of concrete made with high-volume fly ash blended cements using a coarse fly ash, Cem Concr Res. 31(3) (2001) 1393-1402.

[15] M. Olivia, H. Nikraz, Properties of fly ash geopolymer concrete designed by Taguchi method, Mater Des. (2011) 1-27.

[16] M. Chi, R. Huang, Binding mechanism and properties of alkali-activated fly ash/slag mortars, Constr Build Mater. 40 (2013) 291-298.
[17] M. Albitar, P. Visintin, M.S. MohamedAli, M. Drechsler, Assessing behaviour of fresh and hardened geopolymer concrete mixed with class-F fly ash, J Korean Soc Civil Eng. (2014) 1-11.
[18] C. Shi, J. Qian, high performance cementing materials from industrial slags: a review. Resources, Conservation and Recycling. 29(3) (2000) 195-207.
[19] M. Albitar, M.S. Mohamed Ali, P. Visintin, M. Drechsler, Effect of granulated lead smelter slag on strength of fly ash-based geopolymer concrete, Construction and Building Materials. 83 (2015) 128-135.
[20] Z. Zhang, Y. Zhu, T. Yang, L. Li, H. Zhu, H. Wang, Conversion of local industrial wastes into greener cement through geopolymer technology: A case study of high-magnesium nickel slag, Journal of Cleaner Production. 141 (2017) 463-471.
[21] ASTM C989, Standard Specification for Ground Granulated Blast-Furnace Slag for Use in Concrete. American society for testing and materials. West Conshohocken, PA, USA: ASTM International; 2004.
[22] A. Nazari, S. Riahi, SiO2 nanoparticles' effects on properties of concrete using ground granulated blast furnace slag as binder, Magazine of Concrete Research. 64(4) (2012) 295-306.
[23] S. Liu, Z. Wang, X. Li, Long-term properties of concrete containing ground granulated blast furnace slag and steel slag, Magazine of Concrete Research. 66(21) (2014) 1095–1103.
[24] T. Yang, X. Yao, Z. Zhang, Geopolymer prepared with high-magnesium nickel slag: Characterization of properties and microstructure, Construction and Building Materials. 59 (2014) 188-194.
[25] D. F. Velandia, C. J. Lynsdale, J. L. Provis, F. Ramirez, Effect of mix design inputs, curing and compressive strength on the durability of Na_2SO_4-activated high volume fl y ash concretes, Cement and Concrete Composites. 91(19) (2018) 11–20.
[26] A. K. Saha, M. N. N. Khan, P. K. Sarker, Value added utilization of by-product electric furnace ferronickel slag as construction materials , A review. Resources,Conservation & Recycling. 134 (2018) 10–24.
[27] R. Cao, B. Li, N. You, Y. Zhang, Z. Zhang, Properties of alkali-activated ground granulated blast furnace slag blended with ferronickel slag, Construction and Building Materials. 192 (2018)123–132.
[28] Q. Wang, Z. Huang, D. Wang, Influence of high-volume electric furnace nickel slag and phosphorous slag on the properties of massive concrete, Journal of Thermal Analysis and Calorimetry. 131(2) (2018) 873–885.
[29] A. M. M. Al Bakri, H. Kamarudin, I. K. Nizar, M. Bnhussain, Y. Zarina, A. R. Rafiza, Correlation between Na 2 SiO 3 / NaOH Ratio and Fly Ash / Alkaline Activator Ratio to the Strength of Geopolymer, Adv. Mater. Res. 342 (2012)189–193.
[30] P. Nath, P. K. Sarker, Effect of GGBFS on setting, workability and early strength properties of fly ash geopolymer concrete cured in ambient condition, Construction and Building Materials. 66 (2014) 163-171.

[31] T. Yang, Q.Wu, H. Zhu, Z. Zhang, Geopolymer with improved thermal stability by incorporating high magnesium nickel slag, Construction and Building Materials. 155 (2017) 475–484.
[32] I. Ismail, S.A. Bernal, J.L. Provis, R. San Nicolas, D.G. Brice, A.R. Kilcullen, S. Hamdan, J.S.J.Van Deventer, Influence of fly ash on the water and chloride permeability of alkali-activated slag mortars and concretes, Construction and Building Materials. 48 (2013) 1187–1201.
[33] P. Pavithra, M. S. Reddy, P. Dinakar, B. H. Rao, B. K. Satpathy, A. N. Mohanty, A mix design procedure for geopolymer concrete with fly ash, Journal of Cleaner Production. 133 (2016) 117–125.
[34] M. Sofi, J. S. J. van Deventer, P. A. Mendis, G. C. Lukey, Engineering properties of inorganic polymer concretes (IPCs), Cement and Concrete Research. 37(2) (2007) 251–257.
[35] P. Nath, P. K. Sarker, Flexural strength and elastic modulus of ambient-cured blended low-calcium fly ash geopolymer concrete, Construction Building Materials. 130 (2016) 22–31.
[36] ASTM C496, Standard Test Method for Splitting Tensile Strength of Cylindrical Concrete Specimens, Annu. B. American society for testing and materials, ASTM International; 2011.
[37] G. S. Ryu, Y. B. Lee, K. T. Koh, Y. S. Chung, The mechanical properties of fly ash-based geopolymer concrete with alkaline activators, Construction and Building Materials. 47 (2013) 409–418.
[38] S. Kumar, R. Kumar, Influence of granulated blast furnace slag on the reaction, structure and properties of fly ash based geopolymer, J Mater Sci. 45 (2010) 607–615.
[39] A. Fernandez-Jimenez, I. García-Lodeiro, A. Palomo, Durability of alkali-activated fly ash cementitious materials, J. Mater. Sci. 42(9) (2007) 3055–3065.
[40] S. K. Nath, S. Kumar, Influence of iron making slags on strength and microstructure of fly ash geopolymer, Construction and Building Materials. 38 (2013) 924–930.
[41] S. Alehyen, M. E. L. Achouri, M. Taibi, Characterization, microstructure and properties of fly ash-based geopolymer, J. Mater. Environ. Sci. 8 (5) (2017) 1783–1796.
[42] A. M. Rashad, Properties of Alkali-Activated Fly Ash Concrete, Iranian Journal of Materials Science and Engineering. 10(1) (2013) 57–64.
[43] Z. Yahya, A.M.M. Al Bakri, K. Hussin, K.N. Ismail, A.V. Sandu, P. Vizureanu, A.R. Razak, Chemical and Physical Characterization of Boiler Ash from Palm Oil Industry Waste for Geopolymer Composite, Revista de Chimie. 64(12) (2013) 32–34.
[44] M. Faisal, K. Muhammad, Synthesis and characterization of geopolymer from bagasse bottom ash, waste of sugar industries and naturally available china clay, Journal of Cleaner Production. 129 (2016) 491–495.
[45] S. Ahmari, X. Ren, V. Toufigh, L. Zhang, Production of geopolymeric binder from blended waste concrete powder and fly ash, Construction and Building Materials. 35 (2012) 718–729.
[46] M. Tatzber, M. Stemmer, H. Spiegel, C. Katzlberger, G. Haberhauer, A. Mentler, M.H. Gerzabek, FTIR-spectroscopic characterization of humic acids and humin fractions obtained by advanced NaOH, Na4P2O7, and Na 2CO3 extraction procedures, Journal of Plant Nutrition and Soil Science. 170(4) (2007) 522–529.

[47] K. Komnitsas, D. Zaharaki, V. Perdikatsis, Geopolymerisation of low calcium ferronickel slags, Journal of Materials Science. 42(9) (2007) 3073–3082.
[48] C. Jeyageetha, S. P. Kumar, Study of SEM / EDXS and FTIR for Fly Ash to Determine the Chemical Changes of Ash in Marine Environment, International Journal of Science and Research. 5(7) (2016) 1688–1693.
[49] Z. Yunsheng, S. Wei, C. Qianli, C. Lin, Synthesis and heavy metal immobilization behaviors of slag based geopolymer, Journal of Hazardous Materials. 143 (2007) 206–213.
[50] A. Fernández-Jiménez, F. Puertas, Effect of activator mix on the hydration and strength behaviour of alkali-activated slag cements, Advances in Cement Research. 15(3) (2003) 129–136.
[51] C.Y. Heah, Y.M. Liew, A. M. M, Al Bakri, Thermal Resistance Variations of Fly Ash Geopolymers : Foaming Responses, Scientific Reports. 7 (2017) 453-55.
[52] J. Davidovits, Properties of geopolymer cements, International conference on Alkaline Cements and Concretes. KIEV Ukr. (1994) 1–19.